

生物可降解介孔硅纳米粒的研究进展

费伟东¹, 陶姣阳², 宋倩倩¹, 赵云春¹, 杨昊堃³, 诸佳珍², 李范珠^{2*}

(1. 浙江大学医学院附属妇产科医院药剂科, 浙江 杭州 310006; 2. 浙江中医药大学药学院, 浙江 杭州 310053; 3. 浙江大学医学院附属妇产科医院妇二科, 浙江 杭州 310006)

摘要: 介孔硅纳米粒具有比表面积大、介孔结构高度有序、表面易修饰及对药物缓控释等特点, 是被广泛用作诊断、治疗药物递送的载体。随着研究的深入, 介孔硅纳米材料的生物可降解性和可代谢性越来越受到关注, 这是纳米制剂向临床转化的先决条件。本文将重点介绍用金属氧化物掺杂法和有机物掺杂法制备生物可降解介孔硅纳米粒, 探讨其降解原理及降解过程, 并展望新型可降解介孔硅纳米粒在递药系统构建方面的应用前景。

关键词: 生物可降解; 介孔硅纳米粒; 金属氧化物掺杂法; 有机物掺杂法; 降解机制

中图分类号: R943

文献标识码: A

文章编号: 0513-4870 (2018) 05-0716-11

Advance in research of biodegradable mesoporous silica nanoparticles

FEI Wei-dong¹, TAO Jiao-yang², SONG Qian-qian¹, ZHAO Yun-chun¹, YANG Hao-kun³,
ZHU Jia-zhen², LI Fan-zhu^{2*}

(1. Department of Pharmacy, Women's Hospital, School of Medicine, Zhejiang University, Hangzhou 310006, China; 2. College of Pharmaceutical Science, Zhejiang Chinese Medical University, Hangzhou 310053, China; 3. Second Department of Gynecology, Women's Hospital, School of Medicine, Zhejiang University, Hangzhou 310006, China)

Abstract: Mesoporous silica nanoparticles (MSNs) have been widely used as drug carriers in the diagnosis and treatment of diseases due to their specific characteristics, which include a large surface area, ordered mesoporous structures, easy surface modification and feasible sustained release action for encapsulated drugs. With the research development of MSNs, the biodegradability and removability of mesoporous silica nanomaterials have attracted considerable attention in the clinical application of the MSNs-based formulations. This paper was prepared to emphasize the preparation approaches of biodegradable mesoporous silica nanoparticles through the metal oxide doping method and the organic compound doping method. We discussed the biodegradable mechanism and process of such nanoparticles, and finally, provided an insightful and helpful review of the prospective application of the biodegradable mesoporous silica nanoparticles in medical field.

Key words: biodegradability; mesoporous silica nanoparticles; metal oxide doping method; organic compound doping method; biodegradable mechanism

近年来, 无机纳米材料具有理想的生物相容性、低免疫原性、对脂肪酶和胆汁盐的耐受性等特性, 在医药领域备受关注^[1, 2]。其中介孔二氧化硅纳米粒

(mesoporous silica nanoparticles, MSNs) 因比表面积和孔容积大, 表面易修饰及对药物缓控释等优势, 已成为热门的递药载体^[3-5]。作者前期研究中所合成的球状 (mobile crystalline material-41, MCM-41)^[6]、中空型 (hollow mesoporous silica nanoparticles, HMSNs)^[7]及棒状 (santa barbara amorphous-15, SBA-15)^[8]三种不同类型的介孔硅纳米粒 (图 1A~C) 分别对难溶性有机小分子紫杉醇 (paclitaxel, PTX)、无机小分子药物三氧化二砷 (arsenic trioxide, ATO)

收稿日期: 2017-11-27; 修回日期: 2017-12-21.

基金项目: 国家自然科学基金资助项目 (81473361, 81673607); 浙江省中医药优秀青年人才基金资助项目 (2018ZQ013).

*通讯作者 Tel: 86-571-86633030, Fax: 86-571-86613607,

E-mail: lifanzhu@zcmu.edu.cn

DOI: 10.16438/j.0513-4870.2017-1181

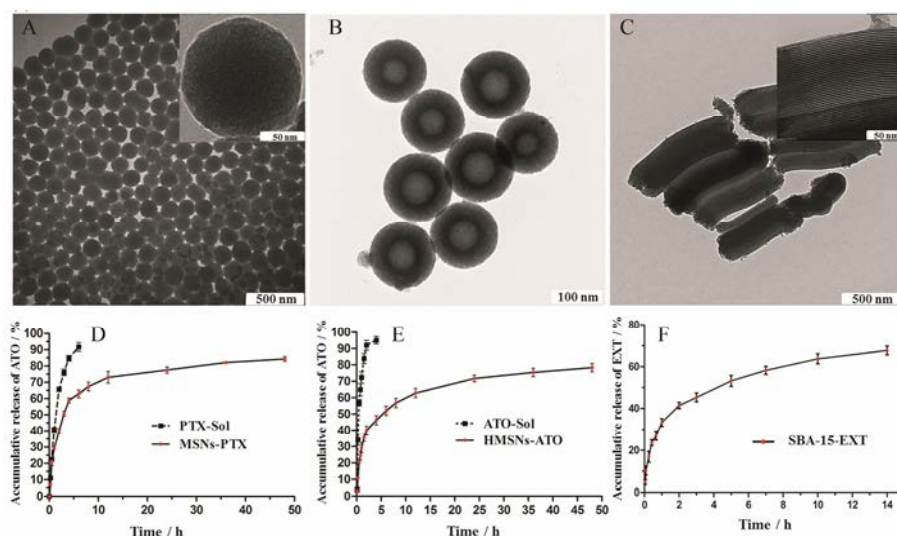


Figure 1 Transmission electron microscope (TEM) images of three different types of mesoporous silica nanoparticles: mobile crystalline material-41 (MCM-41) (A); hollow mesoporous silica nanoparticles (HMSNs) (B); santa barbara amorphous-15 (SBA-15) (C). *In vitro* release profiles of paclitaxel (PTX) (D), arsenic trioxide (ATO) (E) and exenatide (EXT) (F) from MCM-41, HMSNs and SBA-15, respectively^[6-8]

及蛋白类药物艾塞那肽 (exenatide, EXT) 具有较理想的载药量并展现了优越的缓控释作用 (图 1D~F)。然而, 传统 MSNs 中稳定的-Si-O-Si-骨架结构在生物体内降解十分缓慢 (大于 3 周)^[9,10], 并且容易在肝、肾、脾、肺和膀胱等机体重要器官聚集^[11,12], 继而引发严重的炎症反应、氧化损伤及器官纤维化等不良反应^[13,14]。此外, Yamashita 等^[15]发现, 在小鼠体内, 70 nm 左右的 MSNs 通过胎盘滋养细胞后被胚胎肝细胞和脑细胞所摄取, 在胎鼠体内蓄积并严重影响其生长发育, 高浓度时甚至引起其他并发症。综上, MSNs 的难降解性与蓄积毒性已经严重阻碍了它们向临床转化的进程。

目前, 国内外多个团队研制出生物可降解介孔硅纳米粒, 不但保留了介孔材料在递药与释药方面的优势, 而且能够在生物体内迅速降解并代谢, 有效降低了体内蓄积毒性。本文旨在介绍生物可降解介孔硅纳米粒的制备, 从骨架结构变化的角度阐述其降解特性, 并展望此类载体在生物医药领域的应用前景。

1 生物可降解介孔硅纳米粒的特点

随着材料科学的迅速发展, 许多研究团队将新型生物材料修饰到介孔硅纳米粒的内/外表面, 赋予了递药系统生物内环境响应释放药物的特性, 如 pH 敏感型^[16,17]、氧化还原敏感型^[18,19]和酶敏感型^[20,21]释药等。此类递药系统的共同特点是拥有生物环境响应切割的化学键。与之类似, 现有报道的生物可降解介孔硅纳米粒是在原来的-Si-O-Si-骨架中共价掺入

生物体内环境可切割的化学基团, 或在-Si-O-Si-骨架形成过程中非共价掺入有机化合物分子, 从而导致所构建的介孔硅纳米粒骨架结构缩合度降低, 孔隙度增加, 加速纳米粒在生物体内环境中的溶蚀速度, 最终导致其迅速降解。通过此类思路制备的生物可降解介孔硅纳米粒与 MSNs 空间结构相似, 因此, 对药物仍然具有较高的载药量及缓控释特性。此外, 因递药系统的降解, 药物能实现更彻底地释放。

2 金属氧化物掺杂的可降解介孔硅纳米粒

在 MSNs 的-Si-O-Si-骨架中掺入金属氧化物能调节纳米粒的水解/降解速率。所掺杂的金属氧化物的水解稳定性将影响纳米骨架的稳定性及二氧化硅溶解成硅酸的速率。本部分介绍了氧化钙、氧化锰和氧化铁 3 种金属氧化物掺杂的可降解介孔硅纳米粒的合成及其生物可降解特性。

2.1 氧化钙掺杂的可降解介孔硅纳米粒 钙元素掺杂的介孔硅材料通常被用于骨损伤修复等骨组织工程领域^[22-24]。研究发现, 氧化钙掺杂的硅纳米粒 (calcium oxide doped hollow mesoporous silica nanoparticles, Ca-MSNs) 在水性分散体系中的水解/降解速率显著高于 MSNs^[25-27]。施剑林团队^[28]通过向十六烷基三甲基溴化铵 (表面活性剂) 碱性水溶液中加入硝酸钙和磷酸三乙酯, 然后与原硅酸四乙酯 (tetraethyl orthosilicate, TEOS) 反应, 首次合成了 Ca-MSNs。通过表征, Ca-MSNs 中含 8% 氧化钙, 孔容积为 $770 \text{ m}^3 \cdot \text{g}^{-1}$, 具有较高的孔隙率。Ca-MSNs 在 37°C 的中性水环境中孵育 3 天后, 纳米粒介孔孔道

消失, 大孔数量显著增加, Ca-MSNs 表面结构从圆整逐渐不规则化 (图 2A, B), 通过电感耦合等离子体原子发射光谱法监测 Ca^{2+} 浸出约 40% (图 2C)。上述现象均由 Ca-MSNs 降解所致。与此同时, Ca-MSNs 上清液中硅的含量较 MSNs 显著升高, 说明钙离子的浸出有利于硅骨架的降解/水解 (图 2D)。二氧化硅在水中的溶解包括水合、水解和离子交换 3 个过程^[29]。带硅醇基的硅酸盐在水性溶液环境中形成四面体结构 $[(\text{SiO}_4)^4-]$, 然后受到亲核基团 (主要为 OH^-) 的攻击, 形成不稳定的 5 配位中间体, 最终 Si-O-Si 键断裂, 中间体分解成 Si-O^- 和 $\text{Si}(\text{OH})_4$ ^[28]。在 MSNs 中, 上述水解反应被致密的网络结构导致的空间位阻所抑制, 而在 Ca-MSNs 中, Ca-O 易在酸性环境中断裂, Ca^{2+} 从 Si-O-Ca-O-Si 的结构中离去, 形成了结构缺陷并产生大量的活性硅醇基, 使硅更容易重排进入 5 配位中间体, 从而加速了纳米骨架的水解。

张金超团队^[25]进行了可降解介孔硅纳米粒递送多柔比星 (doxorubicin, DOX) 的研究 (图 3A)。研究者通过粉末衍射、红外光谱和 X 射线光电子能谱证明了 Ca-MSNs 中存在 Si-O-Ca-O-Si 结构域。研究所制备 Ca-MSNs 的比表面积为 $543 \text{ m}^2 \cdot \text{g}^{-1}$ 。在 pH 7.4 和 5.0 环境中, Ca-MSNs 逐渐释放出钙离子 (图 3B), 其中 Ca-MSNs 在 pH 5.0 环境中钙离子的释放度约是 pH 7.4 环境中的 100 倍。透射电子显微镜 (transmission electron microscope, TEM) 图像显示: 在 pH 5.0 环境

中, Ca-MSNs 在 12 h 内逐渐降解成 5~30 nm 碎片 (图 3C~G)。值得注意的是, Ca-MSNs 的 pH 敏感骨架降解作用使得药物在肿瘤部位释放更加彻底。因此, 载 DOX 的 Ca-MSNs 展现出比 DOX 溶液和载 DOX 的 MSNs 更为理想的抗肿瘤效果。动物安全性研究结果表明, Ca-MSNs 处理组 Si 元素在肾脏累积量显著高于普通 MSNs 处理组, Ca-MSNs 处理组小

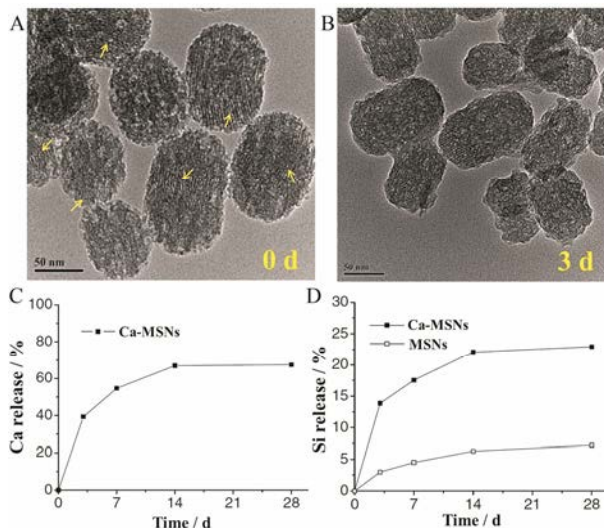


Figure 2 TEM images of calcium oxide doped hollow mesoporous silica nanoparticles (Ca-MSNs) (A) and the degradation product of Ca-MSNs after 3 days (yellow arrows indicated the mesoporous channels) (B). Degradation behavior of mesoporous silica nanoparticles (MSNs) (C) and Ca-MSNs (D) in water^[28]

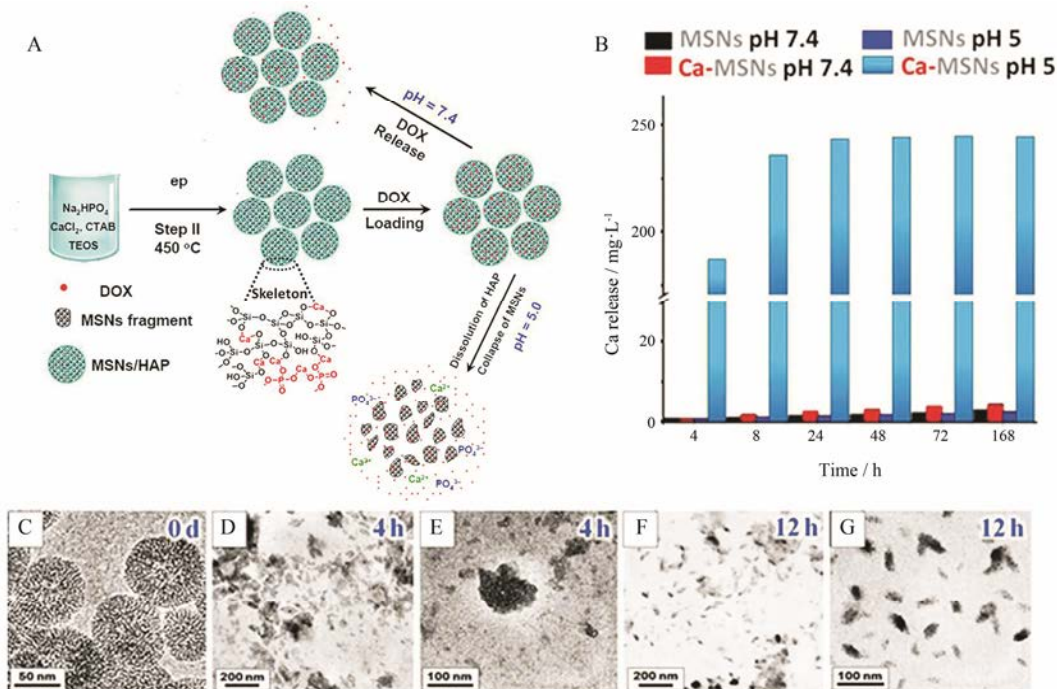


Figure 3 Synthesis and application of Ca-MSNs degradable carriers (A). Quantification of the calcium release from Ca-MSNs and MSNs at different pH (B). TEM images before and after degradation over time of Ca-MSNs (C-G)^[25]. DOX: Doxorubicin

鼠尿液中含有更多的荧光标记的纳米碎片。因为直径小于 5.5 nm 的无机纳米粒容易通过肾脏清除^[30], Ca-MSNs 降解后, 更多的小片段积聚在肾脏, 通过肾脏清除排出体外。该研究证明机体对 Ca-MSNs 具有更高的代谢和排泄能力。

2.2 氧化锰掺杂的可降解介孔硅纳米粒 锰是人体代谢的必需元素之一, 具有毒性低、生物安全性高和易代谢等特点。有研究将氧化锰引入介孔硅纳米粒^[31], 从而调控递药系统在肿瘤微环境中的降解性。研究者 MSNs 的分散体系中加入一水合硫酸锰 ($8 \text{ g}\cdot\text{L}^{-1}$)

和马来酸二钠 ($10 \text{ g}\cdot\text{L}^{-1}$), 于 $180 \text{ }^\circ\text{C}$ 水热处理 12 h, 制备氧化锰掺杂的中空介孔硅纳米粒 (manganese oxide doped hollow mesoporous silica nanopartilces, Mn-HMSNs) (图 4A, B), 其中锰元素掺杂量为 9.4% (Wt%)。Mn-HMSNs 的比表面积、孔体积和平均孔径分别为 $222 \text{ m}^2\cdot\text{g}^{-1}$, $0.53 \text{ cm}^3\cdot\text{g}^{-1}$ 和 3.8 nm 。通过电感耦合等离子光谱仪和能谱仪测定体外降解反应中 Mn 和 Si 的溶出量 (图 4C, D): 在 pH 5.0 及生物还原剂谷胱甘肽 (glutathione, GSH) 存在的条件下, Mn-HMSNs 在 12 h 内释放约 50% 锰元素和 20% 硅元

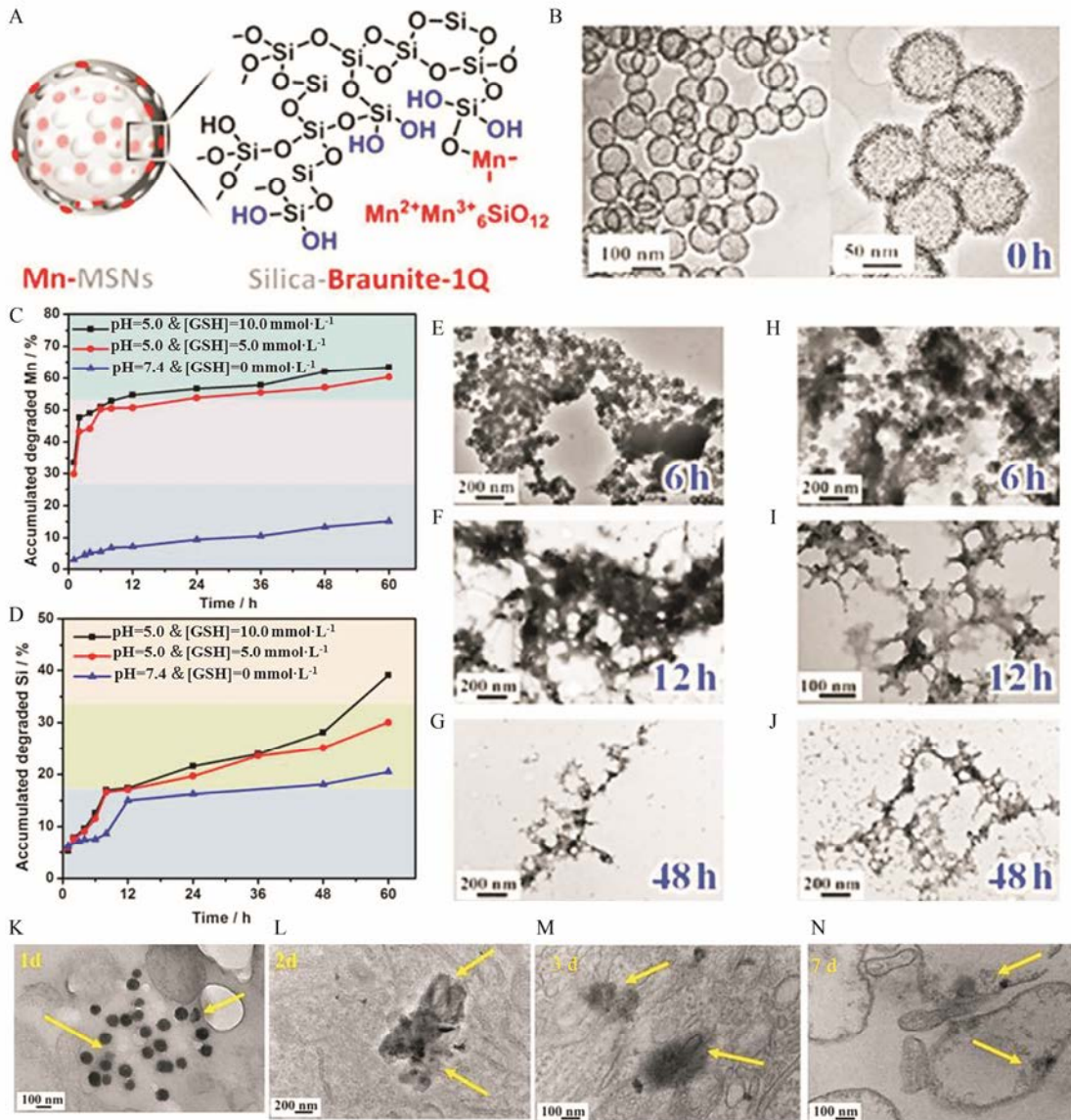


Figure 4 Representation of the possible structure of manganese oxide doped hollow mesoporous silica nanopartilces (Mn-HMSNs) composed of braunite-1Q (A) and their TEM images (B). Accumulated releasing profiles of Mn (C) and Si (D) elements in SBF at different glutathione (GSH) concentrations (5.0 or $10 \times 10^{-3} \text{ mol}\cdot\text{L}^{-1}$) under different pH condition. TEM images showing the structural evolution of Mn-HMSNs after the biodegradation at the GSH concentration of $5.0 \times 10^{-3} \text{ mol}\cdot\text{L}^{-1}$ (E-G) and $10.0 \times 10^{-3} \text{ mol}\cdot\text{L}^{-1}$ (H-J) under pH 5.0. Bio-TEM images of cells after co-incubation with Mn-HMSNs to observe the intracellular biodegradation behavior of Mn-HMSNs (K-N)^[31]

素; 12~48 h 是骨架降解的平台期, 在此期间纳米粒由大颗粒逐渐降解成小颗粒; 48 h 后, 因小颗粒降解更加迅速, 硅元素溶出速率进一步加快。TEM 结果显示, 在 GSH 溶液环境中, 介孔硅纳米粒在 48 h 内几乎全部降解为纳米碎片 (图 4E~J)。Mn-O 键是一种酸和还原性敏感的化学键, 能特异性地在酸性和还原性环境中断裂^[32], 使锰离子游离到溶液中。锰离子从框架中的浸出使得介孔硅纳米网络中产生结构缺陷与大量硅醇基, 进一步诱导/加速了氧化硅骨架的生物水解。通过生物 TEM 图像 (图 4K~N) 发现癌细胞中 Mn-HMSNs 在 7 天内几乎全部降解; 体内安全性研究表明, 48 h 内荷瘤小鼠肝脏、脾脏、肾脏

和肿瘤中的 Mn-HMSNs 基本清除。此外, Mn-HMSNs 在肿瘤微环境中的降解能够导致药物释放并引发 Mn²⁺ 的 T₁ 加权磁共振成像。

2.3 氧化铁掺杂的可降解介孔硅纳米粒 鉴于二氧化硅在氧化铁非均相界面处具有较低的缩合度 (图 5A), 哺乳动物血清中铁的生物配体 (血红蛋白) 与 Fe³⁺ 具有较大的结合常数, 氧化铁掺杂的介孔硅纳米粒 (iron oxide doped mesoporous silica nanoparticles, Fe-MSNs) 因 Fe³⁺ 的溶解或螯合容易从纳米结构中离去, 从而提高了纳米载体的降解性^[33-35]。Trogler 团队^[9]通过溶胶-凝胶法将四甲氧基原硅酸酯和乙醇铁(III) (20 g·L⁻¹) 的混合溶液, 加入到聚苯乙烯与乙

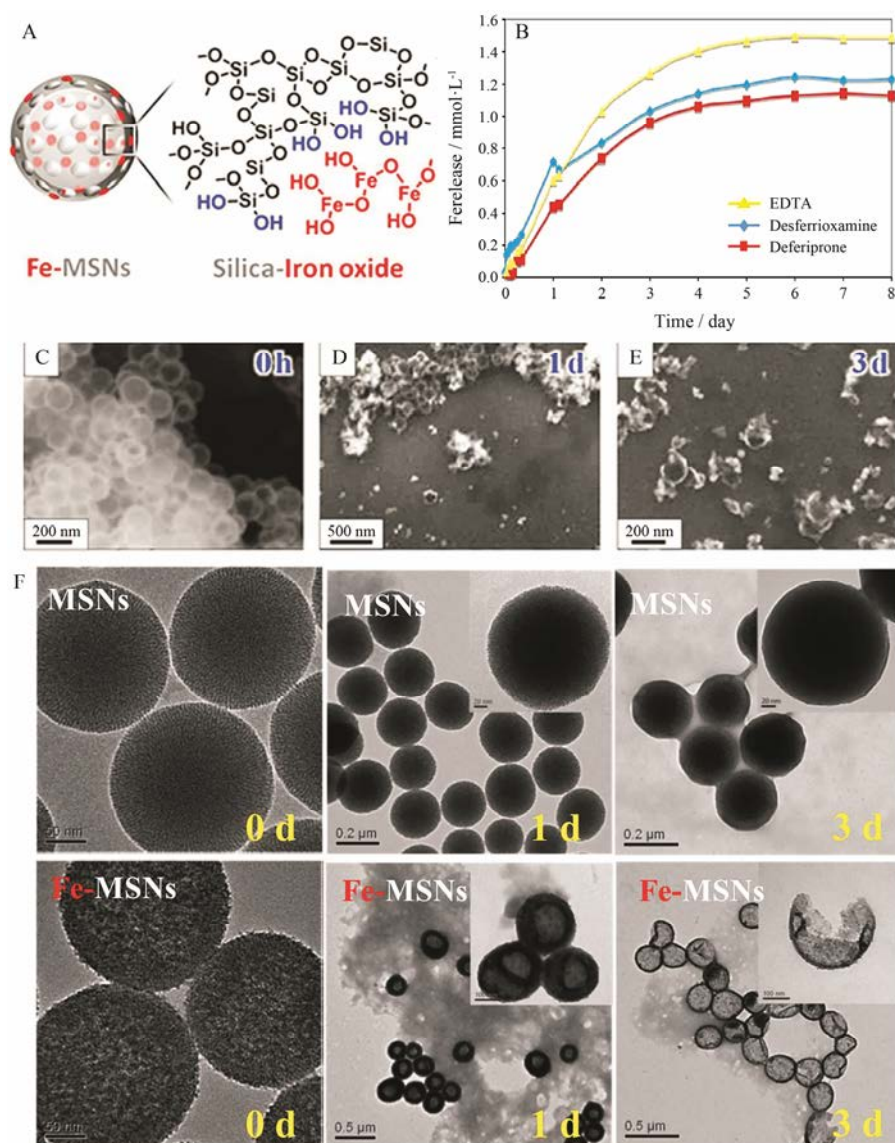


Figure 5 Representation of the possible structure of iron oxide doped mesoporous silica nanoparticles (Fe-MSNs) composed of iron oxide heterogeneous structure (A, the blue color highlights the lower condensation degree at the interfaces of phases). Iron release profile from Fe-MSNs upon various chelating agents (0.1 mol·L⁻¹ aqueous chelating solution of EDTA, desferrioxamine, or deferiprone, B), along with the scanning electron microscope images before (C) and after degradation for 1 day (D) and 3 days (E), facilitated by deferiprone chelation. TEM images of MSNs and Fe-MSNs over time in fetal bovine serum (FBS) solution at 37 °C (F) ^[9, 35]

醇的混合悬浮液中, 搅拌制备得 Fe-MSNs。研究发现: Fe-MSNs 中的铁可以通过不同的螯合剂 (乙二胺四乙酸二钠, EDTA) 除去 (图 5B), 并且随着铁的除去, 纳米粒不断地降解 (图 5C~E)。Fe-MSNs 在血清和胎牛血清 (fetal bovine serum, FBS) 环境中降解约为 20 天。Peng 等^[35]所制备的 Fe-MSNs 在 PBS 中 3 天内出现明显降解 (图 5F), 而在相同情况中, MSNs 依旧保持完整的形态。另有研究表明, Fe-MSNs 中 Fe^{3+} 与内源性转铁蛋白相互作用能促进纳米粒转运进入细胞^[36]。

3 有机物掺杂的可降解介孔硅纳米粒

介孔硅纳米粒的降解速率还可以通过有机化物的掺杂来调节和控制。现有的研究主要采用以下两种策略: ① 有机分子非共价掺杂形成介孔硅纳米粒, 该方法导致硅纳米骨架低聚化, 从而加速其水解/降解^[30, 37, 38]; ② 通过有机硅烷 [如: 双-(三乙氧基甲基硅烷基丙基) 二硫化物, BTSPD] 的水解反应使生理环境可切割的有机基团参与二氧化硅骨架结构形成, 并以此调控介孔硅纳米粒的降解速率。本部分将重点介绍亚甲蓝非共价掺杂、二硫键^[39-41]和酰胺键共价掺杂^[42]的介孔硅纳米粒的合成及其降解特性。

3.1 亚甲蓝非共价掺杂的可降解介孔硅纳米粒

非共价掺杂指有机物与二氧化硅之间没有发生化学反应, 以分子形式堆砌于介孔硅纳米网络结构中, 通过调节硅和氧的缩合密度来调控纳米粒的降解速率。Zhang 等^[30]通过在 TEOS 水解缩合的过程中加入相反电荷的亚甲蓝 (methylene blue, MB), MB 分子与硅酸静电结合成为“核”, 随着 TEOS 的持续水解, 高密度的 MB 堆砌纳米粒内部, 最终制备了 MB 非共价掺杂的可降解介孔硅纳米粒 (MB doped mesoporous silica nanoparticles, MB-MSNs) (图 6A)。2 天内, MB-MSNs 出现了明显的降解 (图 6B), 在模拟体液 (simulated body fluid, SBF) 中释放出近 60% Si (图 6C)。当 MB-MSNs 分散在 MB 可溶性溶剂中, MB 分子被不断萃取到溶剂中, 导致纳米网络孔隙度不断增加, 水解速率随之提高, 最终导致硅纳米粒完全崩解。MB-MSNs 中 MB 的含量越高, 纳米粒降解速率越快。两天内, 约 55% 硅元素通过尿液排出体外 (图 6D), 说明 MB-MSNs 具有较高的生物安全性。然而, 该方法现仅适合于可溶性且与介孔硅纳米粒带相反电荷的有机化合物的掺杂。

3.2 二硫键共价掺杂的可降解介孔硅纳米粒

生物细胞内 GSH 的浓度 ($2 \times 10^{-3} \sim 10 \times 10^{-3} \text{ mol} \cdot \text{L}^{-1}$) 高于细胞外的浓度 ($2 \times 10^{-6} \sim 20 \times 10^{-6} \text{ mol} \cdot \text{L}^{-1}$), 癌细胞中

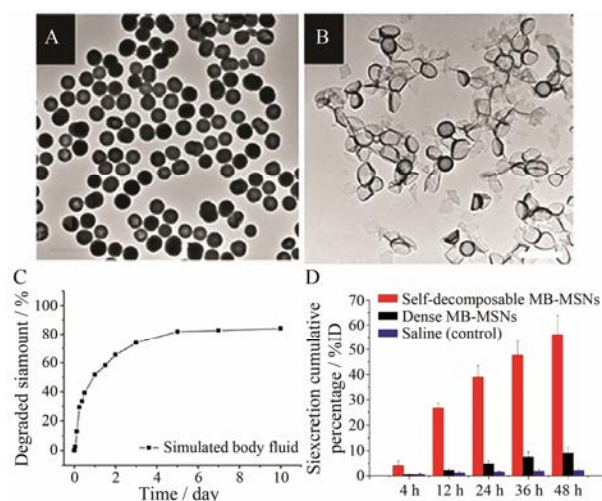


Figure 6 TEM images of the freshly prepared MB doped mesoporous silica nanoparticles (MB-MSNs) (A) and those after being immersed in deionized water for 2 days (B). Inductively coupled plasma optical emission spectrometry (ICP-OES) result of degraded silica amount in simulated body fluid (C). ICP-OES analysis of Si amount in urinary excretion collected at 4, 12, 24, 36 and 48 h after injection of self-decomposable MB-MSNs, dense MB-MSNs or saline (% of the injection dose, %ID) (D)^[30]

GSH 浓度进一步显著高于正常细胞^[43]。二硫化物共价掺杂的纳米递药系统因可被细胞内 GSH 诱导降解而被广泛应用于药物^[44, 45]和基因^[46, 47]的递送。施剑林等^[39, 40]将 TEOS 和 BTSPD 作为硅源, 利用选择性侵蚀法制备了含二硫键的中空介孔有机硅纳米粒 (hollow mesoporous organosilica nanoparticles, HMONS)。HMONS 中-Si-C-键的键长长于-Si-O-键, 表明-Si-C-键的键能低于-Si-O-键; -S-S-键的键长比-Si-C-和-Si-O-键的键长都要长得多, 因此-S-S-的键能最低, 最容易发生断裂 (图 7A)。另外, HMONS 框架内的二硫键对还原微环境具有高度响应性, 二硫键的断裂能够破坏 HMONS 致密的网络结构, 增加了孔隙度, 从而加速了纳米粒的降解 (图 7B)。通过 TEM 观察 SBF 中 HMONS 的结构变化: 前 7 天变化不明显, 14 天后纳米粒基本结构出现降解及崩塌。在低 GSH ($5 \text{ mmol} \cdot \text{L}^{-1}$) 环境中, HMONS 在 7 天内出现明显降解; 在高 GSH ($10 \text{ mmol} \cdot \text{L}^{-1}$) 环境中, 14 天内 HMONS 几乎全部降解 (图 7C)。体内生物安全性研究表明, 长期静脉给予 HMONS 不会引起心、肝、脾、肺和肾等重要器官的病理改变。小鼠的血液和体重指数均与对照组无显著变化, 证明 HMONS 具有较高的生物安全性。

Maggini 等^[48]将 BTSPD 与 TEOS 作为混合硅源, 然后通过改良 Stober 法合成了二硫键桥接的介孔硅纳米粒 (图 8A)。所制备的可降解介孔硅纳米粒在 PBS

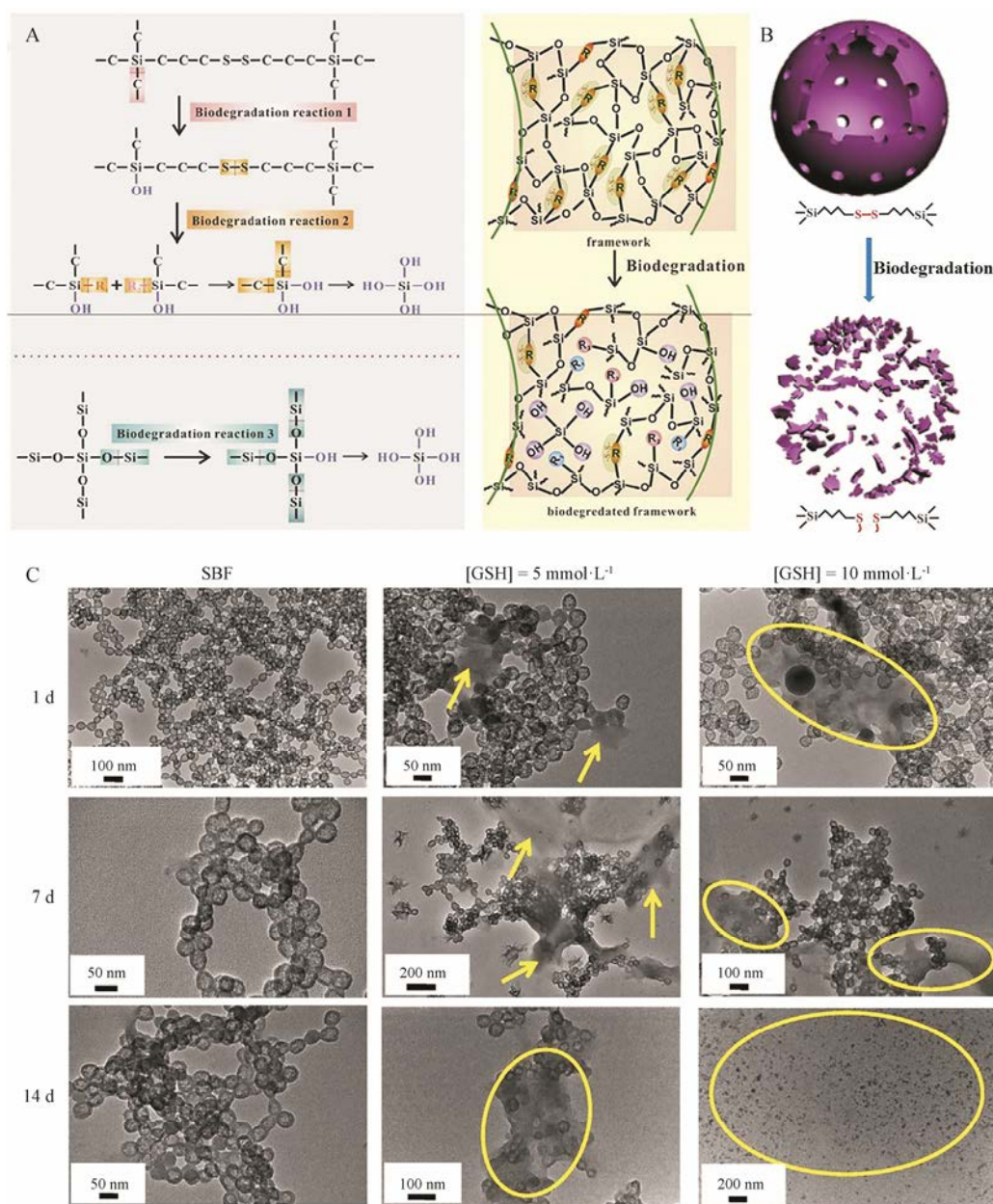


Figure 7 Schematic illustration of three biodegradation reactions involved during the biodegradation process and the scheme of bond-structure change within the framework (A). Nanostructure of hollow mesoporous organic silica nanoparticles (HMONs) and corresponding degradation induced by break-up of physiologically active disulfide bond (-S-S-) within the framework (B). Biodegradation behavior of HMONs in simulated body fluid (C)^[40]

(含 GSH 10 mmol·L⁻¹) 中 7 天内能全部降解 (图 8B), 在生理环境中降解速率高于金属氧化物掺杂的介孔硅纳米粒及选择性侵蚀法所制备的 HMONs。此外, Chang 等^[46]还研究了四硫化物桥接的介孔硅纳米粒的体内外生物可降解特性。

3.3 亚苯基-丙酰胺共价掺杂的可降解介孔硅纳米粒 Fatieiev 等^[49]和 Maggini 等^[50]分别将双(丙基)酰胺基团和赖氨酸直接插入到硅纳米粒骨架中, 所制备的纳米粒在胰蛋白酶环境中展现出良好的生物降解性。上述酶促降解硅纳米粒的研究虽具有开创

性, 但所制备的纳米粒的孔隙度十分低, 并不适合作为递药载体。Croissant 等^[42]通过 1,4-(三乙氧基甲硅烷基)苯和 *N,N'*-双(3-(三乙氧基甲硅烷基)-丙基)草酰胺两种有机硅烷将亚苯基(phenylene)和氧酰胺(oxamide)两种有机基团插入硅纳米粒的骨架中(图 9A), 前者促使介孔的形成, 后者使得所制备的介孔硅纳米粒(oxamide-phenylene mesoporous organosilica nanoparticles, P-OX MONs)可以在胰蛋白酶存在的环境中加速降解(图 9B)。如 TEM 所示, 24 h 时 P-OX MONs 边界模糊化, 视野中出现纳米碎片; 48 h 后,

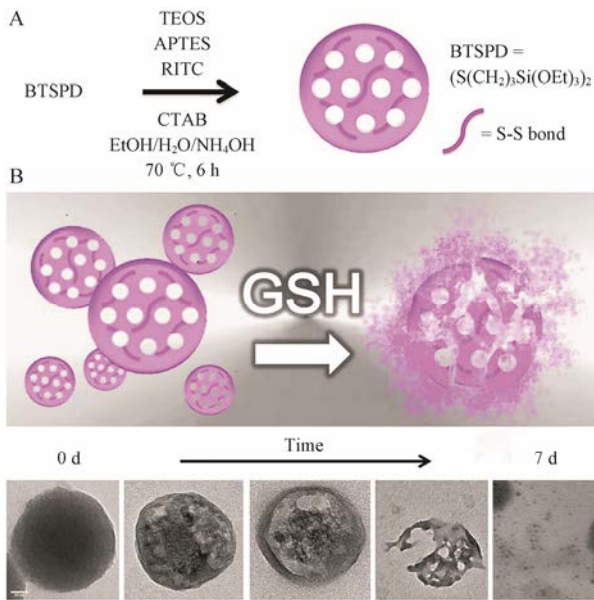


Figure 8 Synthetic route of the breakable disulfide-doped MSNs (A), TEM analysis of a suspension of disulfide-doped MSNs ($0.1 \text{ g} \cdot \text{L}^{-1}$, PBS, $37 \text{ }^\circ\text{C}$) undergoing glutathione (GSH) ($10 \text{ mmol} \cdot \text{L}^{-1}$) reduction (0–7 days) (scale bar = 50 nm) (B)^[48]

纳米粒几乎全部降解 (图 9C, D)。因为生物酶的高效性及丙酰胺结构对酶具有高度敏感性, P-OX MONs 在生理环境中降解速率高于金属氧化物掺杂的介孔硅纳米粒、MB 非共价掺杂的介孔硅纳米粒及二硫

键共价掺杂的介孔硅纳米粒。动态光散射和核磁共振分析进一步证实了 P-OX MONs 的易降解特性 (图 9E~G)。对照实验证明, 亚苯基桥连介孔硅纳米粒 (phenylene mesoporous organosilica nanoparticles, P MONs) 不能在胰蛋白酶环境中降解 (图 9H), P-OX MONs 不能在变性胰蛋白酶降解 (图 9I)。此外, 因 P-OX MONs 的有机成分高 (50%, Wt%), 载体对 DOX 和疏水喜树碱的载药量达到 65% 和 84%, 并且有效缓解介孔材料对药物突释漏释的缺陷。

4 结论与展望

本文综述了可降解介孔硅纳米粒的制备方法及其降解原理。不同金属氧化物的掺杂会影响纳米粒的降解时间: 氧化钙 < 氧化锰 ≈ 氧化铁, 且在酸性条件 (pH 5.0) 下, 金属氧化物掺杂的递药系统的降解比在中性环境中更快。金属-氧键的断裂还能产生大量硅烷醇, 从而进一步诱导/加速骨架的降解。有机硅的共价掺杂赋予了介孔硅纳米粒 GSH 敏感 (二硫化物、四硫化物) 或酶敏感 (酰胺、酯) 裂解的有机基团, 从而实现载体在特定生物环境中的降解。由于有机硅共价掺杂介孔硅纳米粒中环境敏感可切割键的数量远高于金属氧化物掺杂的介孔硅纳米粒中的金属-氧键的数量, 因此前者的降解速率一般高于后者。有机

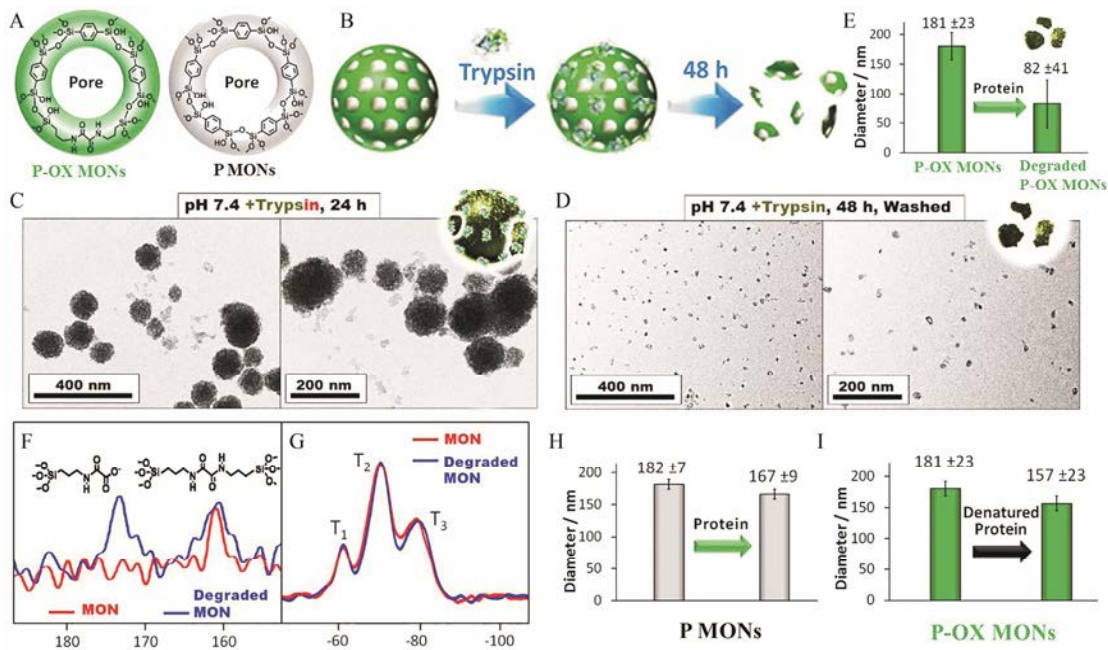


Figure 9 Representation of the pore structure of oxamide-phenylene mesoporous organosilica nanoparticles (P-OX MONs) and phenylene mesoporous organosilica nanoparticles (P MONs) (A). Representation of P-OX MONs and the trypsin-mediated degradation (B). TEM images of P-OX MONs before and after incubation for 24 h (C) and 48 h (D) with trypsin enzyme. Dynamic light scattering analyses of intact and degraded P-OX MONs after stirring with trypsin for 48 h (E). Nuclear magnetic resonance analyses of ^{13}C (F) and ^{29}Si (G) for intact and degraded P-OX MONs. Control dynamic light scattering analyses of intact P MONs mixed with proteins (H), and P-OX MONs mixed with denatured proteins (I)^[42]

物非共价掺杂法制备的可降解介孔硅纳米粒因有机物/药物的溶出而产生了大量结构缺陷,从而加速了纳米骨架的降解,其降解速率与掺杂有机物/药物的溶解性与掺杂的量有关。通过该方法制备的纳米递药系统能够使大部分药物避免肾小球滤过,使有机物/药物在血流中的滞留时间延长^[30]。最终,介孔硅纳米粒降解生成的硅酸盐副产物基本能通过肾脏等排泄器官排出体外,对机体不产生不良反应^[51]。

鉴于各种硅质纳米材料具有不同的物理化学性质、降解和清除动力学,研究人员可以构建特异性纳米平台来满足不同的应用。生物可降解的 Fe-MSNs 和 Mn-HMSNs (通过解离的金属离子共振弛豫) 是生物成像纳米探针的理想选择,也可用于构建“诊疗”一体化纳米药物。金属氧化物掺杂的介孔硅纳米粒所具备的低 pH 或高 GSH 敏感降解的特性使其适合用于构建肿瘤组织特异性释药的纳米递药系统。酶促降解 MSNs 可以设计成靶向药物递送的载体,使纳米递药系统向病灶部位分布,从而实现靶向递药,如有机硅共价掺杂的氧化还原敏感降解型介孔硅纳米粒用于设计成实体瘤靶向递药系统,在解决药物负载问题的同时,可以实现纳米药物在病灶部位的崩解,有效降低硅纳米粒对周围正常组织的蓄积毒性。其他活性蛋白敏感降解的 MSNs 可用于含有特定蛋白质的器官的疾病靶向治疗。研究者还可以通过控制掺杂金属氧化物或有机化合物的比例来调节纳米粒的降解时间,从而满足不同性质药物的释放时间。综上,可降解介孔硅纳米粒不但保留了无机介孔材料在药物负载与递送方面的优势,而且具备了生物降解的特性,在生物医药领域拥有广阔的应用前景。

References

- [1] Dasgupta S, Banerjee SS, Bandyopadhyay A, et al. Zn- and Mg-doped hydroxyapatite nanoparticles for controlled release of protein [J]. *Langmuir*, 2010, 26: 4958–4964.
- [2] Yu Y, Tao C, Yang H, et al. Preparation of mesoporous silica nanoparticles in different pore size and its use in the solidification of sirolimus loaded self-microemulsifying drug delivery system [J]. *Acta Pharm Sin (药学报)*, 2017, 52: 985–991.
- [3] Feng Y, Panwar N, Tng DJH, et al. The application of mesoporous silica nanoparticle family in cancer theranostics [J]. *Coord Chem Rev*, 2016, 319: 86–109.
- [4] Meng H, Liang M, Xia T, et al. Engineered design of mesoporous silica nanoparticles to deliver doxorubicin and P-glycoprotein siRNA to overcome drug resistance in a cancer cell line [J]. *ACS Nano*, 2010, 4: 4539–4550.
- [5] Lee AL, Gee CT, Weegman BP, et al. Oxygen sensing with perfluorocarbon-loaded ultraporos mesostructured silica nanoparticles [J]. *ACS Nano*, 2017, 11: 5623–5632.
- [6] Xiao X, Liu Y, Guo M, et al. pH-Triggered sustained release of arsenic trioxide by polyacrylic acid capped mesoporous silica nanoparticles for solid tumor treatment *in vitro* and *in vivo* [J]. *J Biomater Appl*, 2016, 31: 23–35.
- [7] Fei W, Zhang Y, Han S, et al. RGD conjugated liposome-hollow silica hybrid nanovehicles for targeted and controlled delivery of arsenic trioxide against hepatic carcinoma [J]. *Int J Pharm*, 2017, 519: 250–262.
- [8] Chen C, Zheng H, Xu J, et al. Sustained-release study on exenatide loaded into mesoporous silica nanoparticles: *in vitro* characterization and *in vivo* evaluation [J]. *DARU*, 2017, 25: 20.
- [9] Pohaku Mitchell KK, Liberman A, Kummel AC, et al. Iron(III)-doped, silica nanoshells: a biodegradable form of silica [J]. *J Am Chem Soc*, 2012, 134: 13997–14003.
- [10] Alexis F, Pridgen E, Molnar LK, et al. Factors affecting the clearance and biodistribution of polymeric nanoparticles [J]. *Mol Pharm*, 2008, 5: 505–515.
- [11] He QJ, Shi JL. Mesoporous silica nanoparticle based nano drug delivery systems: synthesis, controlled drug release and delivery, pharmacokinetics and biocompatibility [J]. *J Mater Chem*, 2011, 21: 5845–5855.
- [12] Huang XL, Li LL, Liu TL, et al. The shape effect of mesoporous silica nanoparticles on biodistribution, clearance, and biocompatibility *in vivo* [J]. *ACS Nano*, 2011, 5: 5390–5399.
- [13] Nabeshi H, Yoshikawa T, Matsuyama K, et al. Amorphous nanosilica induce endocytosis-dependent ROS generation and DNA damage in human keratinocytes [J]. *Part Fibre Toxicol*, 2011, 8: 1.
- [14] Nabeshi H, Yoshikawa T, Matsuyama K, et al. Systemic distribution, nuclear entry and cytotoxicity of amorphous nanosilica following topical application [J]. *Biomaterials*, 2011, 32: 2713–2724.
- [15] Yamashita K, Yoshioka Y, Higashisaka K, et al. Silica and titanium dioxide nanoparticles cause pregnancy complications in mice [J]. *Nat Nanotechnol*, 2011, 6: 321–328.
- [16] Cheng W, Liang CY, Xu L, et al. TPGS-functionalized polydopamine-modified mesoporous silica as drug nanocarriers for enhanced lung cancer chemotherapy against multidrug resistance [J]. *Small*, 2017, 13: 1700623.
- [17] Wen J, Yang K, Liu FY, et al. Diverse gatekeepers for mesoporous silica nanoparticle based drug delivery systems

- [J]. Chem Soc Rev, 2017, 46: 6024–6045.
- [18] Han L, Zhang XY, Wang YL, et al. Redox-responsive theranostic nanoplatfoms based on inorganic nanomaterials [J]. J Control Release, 2017, 259: 40–52.
- [19] Chen L, Zhou XJ, Nie W, et al. Multifunctional redox-responsive mesoporous silica nanoparticles for efficient targeting drug delivery and magnetic resonance imaging [J]. ACS Appl Mater Interfaces, 2016, 8: 33829–33841.
- [20] Baeza A, Guisasola E, Torres-Pardo A, et al. Hybrid enzyme-polymeric capsules/mesoporous silica nanodevice for *in situ* cytotoxic agent generation [J]. Adv Funct Mater, 2014, 24: 4625–4633.
- [21] Liu J, Li QL, Zhang JX, et al. Safe and effective reversal of cancer multidrug resistance using sericin-coated mesoporous silica nanoparticles for lysosome-targeting delivery in mice [J]. Small, 2017, 13: 1602567.
- [22] Díaz A, López T, Manjarrez J, et al. Growth of hydroxyapatite in a biocompatible mesoporous ordered silica [J]. Acta Biomater, 2006, 2: 173–179.
- [23] Xia W, Chang J. Well-ordered mesoporous bioactive glasses (MBG): a promising bioactive drug delivery system [J]. J Control Release, 2006, 110: 522–530.
- [24] Lin K, Liu Y, Huang H, et al. Degradation and silicon excretion of the calcium silicate bioactive ceramics during bone regeneration using rabbit femur defect model [J]. J Mater Sci Mater Med, 2015, 26: 1–8.
- [25] Hao X, Hu X, Zhang C, et al. Hybrid mesoporous silica-based drug carrier nanostructures with improved degradability by hydroxyapatite [J]. ACS Nano, 2015, 9: 9614–9625.
- [26] Latifi SM, Fathi MH, Golozar MA. Preparation and characterisation of bioactive hydroxyapatite-silica composite nanopowders *via* sol-gel method for medical applications [J]. Adv Appl Ceram, 2011, 110: 8–14.
- [27] Musa M, Kannan TP, Masudi SM, et al. Assessment of DNA damage caused by locally produced hydroxyapatite-silica nanocomposite using comet assay on human lung fibroblast cell line [J]. Mol Cell Toxicol, 2012, 8: 53–60.
- [28] Li X, Zhang L, Dong X, et al. Preparation of mesoporous calcium doped silica spheres with narrow size dispersion and their drug loading and degradation behavior [J]. Micropor Mesopor Mat, 2007, 102: 151–158.
- [29] Bunker BC. Molecular mechanisms for corrosion of silica and silicate glasses [J]. J Non-Cryst Solids, 1994, 179: 300–308.
- [30] Zhang SL, Chu ZQ, Yin C, et al. Controllable drug release and simultaneously carrier decomposition of SiO₂-drug composite nanoparticles [J]. J Am Chem Soc, 2013, 135: 5709–5716.
- [31] Yu LD, Chen Y, Wu MY, et al. "Manganese extraction" strategy enables tumor-sensitive biodegradability and theranostics of nanoparticles [J]. J Am Chem Soc, 2016, 138: 9881–9894.
- [32] Zhao Z, Wang X, Zhang Z, et al. Real time monitoring of arsenic trioxide release and delivery by activatable T₁ miaging [J]. ACS Nano, 2015, 9: 2749–2759.
- [33] Wang L, Huo M, Chen Y, et al. Iron-engineered mesoporous silica nanocatalyst with biodegradable and catalytic framework for tumor-specific therapy [J]. Biomaterials, 2018, 163: 1–13.
- [34] Peng YK, Tseng YJ, Liu CL, et al. One-step synthesis of degradable T₁-FeOOH functionalized hollow mesoporous silica nanocomposites from mesoporous silica spheres [J]. Nanoscale, 2015, 7: 2676–2687.
- [35] Peng YK, Liu CL, Chen HC, et al. Antiferromagnetic iron nanocolloids: a new generation *in vivo* T₁ MRI contrast agent [J]. J Am Chem Soc, 2013, 135: 18621–18628.
- [36] Mitchell KKP, Sandoval S, Cortes-Mateos MJ, et al. Self-assembled targeting of cancer cells by iron(III)-doped, silica nanoparticles [J]. J Mater Chem B, 2014, 2: 8017–8025.
- [37] Chu ZQ, Zhang SL, Yin C, et al. Designing nanoparticle carriers for enhanced drug efficacy in photodynamic therapy [J]. Biomater Sci, 2014, 2: 827–832.
- [38] Zhao SS, Zhang SL, Ma J, et al. Double loaded self-decomposable SiO₂ nanoparticles for sustained drug release [J]. Nanoscale, 2015, 7: 16389–16398.
- [39] Chen Y, Meng Q, Wu M, et al. Hollow mesoporous organosilica nanoparticles: a generic intelligent framework-hybridization approach for biomedicine [J]. J Am Chem Soc, 2014, 136: 16326–16334.
- [40] Huang P, Chen Y, Lin H, et al. Molecularly organic/inorganic hybrid hollow mesoporous organosilica nanocapsules with tumor-specific biodegradability and enhanced chemotherapeutic functionality [J]. Biomaterials, 2017, 125: 23–37.
- [41] Croissant J, Cattoën X, Man MW, et al. Biodegradable ethylene-bis(propyl)disulfide-based periodic mesoporous organosilica nanorods and nanospheres for efficient *in-vitro* drug delivery [J]. Adv Mater, 2014, 26: 6174–6180.
- [42] Croissant JG, Fatieiev Y, Julfakyan K, et al. Biodegradable oxamide-phenylene-based mesoporous organosilica nanoparticles with unprecedented drug payloads for delivery in cells [J]. Chem Eur J, 2016, 22: 14806–14811.
- [43] Russo A, Degraff W, Friedman N, et al. Selective modulation of glutathione levels in human normal *versus* tumor cells and subsequent differential response to chemotherapy drugs [J]. Cancer Res, 1986, 46: 2845–2848.
- [44] Croissant JG, Qi C, Mongin O, et al. Disulfide-gated mesoporous silica nanoparticles designed for two-photon-triggered drug release and imaging [J]. J Mater Chem B,

- 2015, 3: 6456–6461.
- [45] Xu Z, Zhang K, Liu X, et al. A new strategy to prepare glutathione responsive silica nanoparticles [J]. RSC Adv, 2013, 3: 17700–17702.
- [46] Cheng R, Feng F, Meng F, et al. Glutathione-responsive nano-vehicles as a promising platform for targeted intracellular drug and gene delivery [J]. J Control Release, 2011, 152: 2–12.
- [47] Bauhuber S, Hozsa C, Breunig M, et al. Delivery of nucleic acids *via* disulfide-based carrier systems [J]. Adv Mater, 2009, 21: 3286–3306.
- [48] Maggini L, Cabrera I, Ruiz-Carretero A, et al. Breakable mesoporous silica nanoparticles for targeted drug delivery [J]. Nanoscale, 2016, 8: 7240–7247.
- [49] Fatieiev Y, Croissant JG, Julfakyan K, et al. Enzymatically degradable hybrid organic-inorganic bridged silsesquioxane nanoparticles for *in vitro* imaging [J]. Nanoscale, 2015, 7: 15046–15050.
- [50] Maggini L, Travaglini L, Cabrera I, et al. Biodegradable peptide-silica nanodonuts [J]. Chemistry, 2016, 22: 3697–2703.
- [51] Dove PM, Han N, Wallace AF, et al. Kinetics of amorphous silica dissolution and the paradox of the silica polymorphs [J]. Proc Natl Acad Sci U S A, 2008, 105: 9903–9908.